Supporting Information for

Unraveling the Mechanism of Near-Infrared Thermally Activated Delayed Fluorescence of TPA-based Molecules: Effect of Hydrogen Bond Steric Hindrance

Can Leng[1,2,3], Sheng You[3], Yubing Si[4]*, Hai-Mei Qin[5], Jie Liu[1,2], Wei-Qing Huang[6], Keqin Li[7,8]*

[1]*Science and Technology on Parallel and Distributed Processing Laboratory, National University of Defense Technology, Changsha 410073, China*
[2]*Laboratory of Software Engineering for Complex Systems, National University of Defense Technology, Changsha 410073, China*
[3]*National Supercomputer Center in Changsha, 410082, China*
[4]*College of Chemistry, Zhengzhou University, Zhengzhou, 450001, China*
[5]*College of Chemistry and Chemical Engineering, Fujian Provincial Key Laboratory of Theoretical and Computational Chemistry, Xiamen University, Xiamen 361005, China*
[6] *Department of Applied Physics, School of Physics and Electronics, Hunan University, Changsha* 410082, China
[7] *College of Computer Science and Electronic Engineering, Hunan University, Changsha 410082, China*
[8]*Department of Computer Science, State University of New York, New Paltz, New York 12561, USA*

* ybsi@zzu.edu.cn
* lik@newpaltz.edu

1. Mechanism of electron transfer process on potential energy surface.

2. The comparison of the calculated spectrum and the experimental spectrum.

3. Analysis of electronic excited states distribution.

4. The dihedral angle Φ of C_1-C_2-C_3-C_4 and its comparison between the ground state and the excited states of two TADF molecules.

1. Mechanism of electron transfer process on potential energy surface.

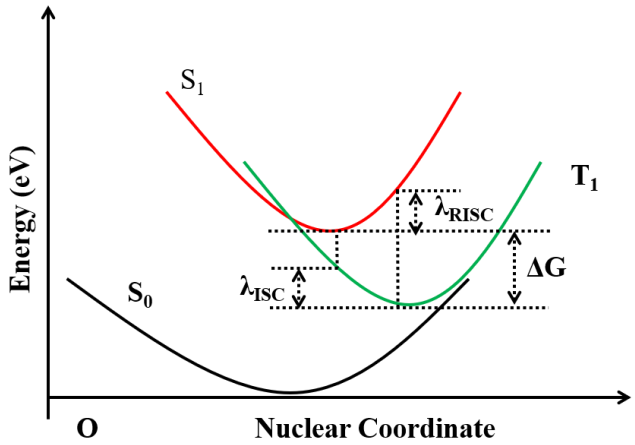

Figure S1. Potential energy surface of S_0, S_1 and T_1. The state for S_1 and T_1 and its electron transfer process by ISC and RISC, as well as the three Marcus parameters, are shown in the scheme.

2. The comparison of the calculated spectrum and the experimental spectrum.

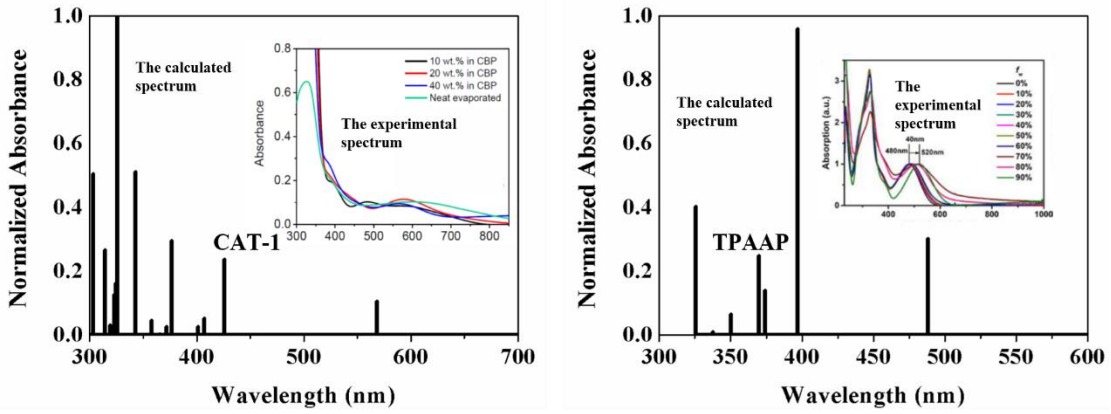

Figure S2. The oscillation strengths of vertical excitations in the two TADF molecules at the B3LYP/def2-SVP level. (a) the comparison of the calculated spectrum and the experimental spectrum[1] in toluene solution for CAT-1molecule; (b) the comparison of the calculated spectrum and the experimental spectrum[2] in toluene solution for TPAAP molecule;

3. Analysis of electronic excited states distribution.

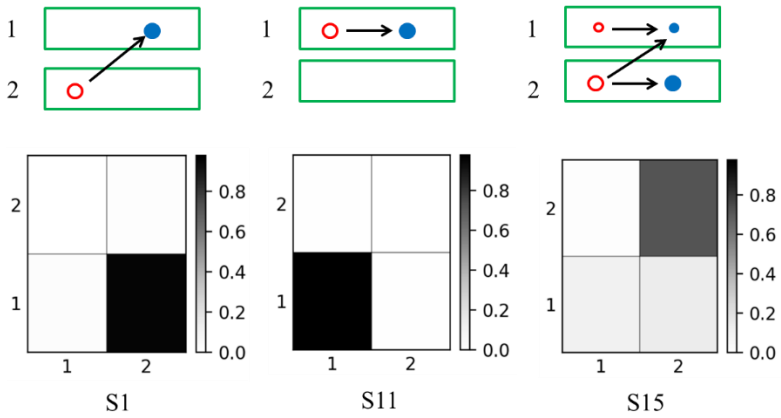

Figure S3. Different types of excited states distributed over three coupled fragments for CAT-1. (a) electron transfer from Donor 2 to Acceptor 1, (b)local excitation on Acceptor 1, (c) Local excitation on Donor 2 and Acceptor 1, as well as the electron transfer from 2 to 1. Top: graphical representation of the distribution of the hole (red) and electron (blue) over the fragments; bottom: analysis via electron-hole correlation plots.

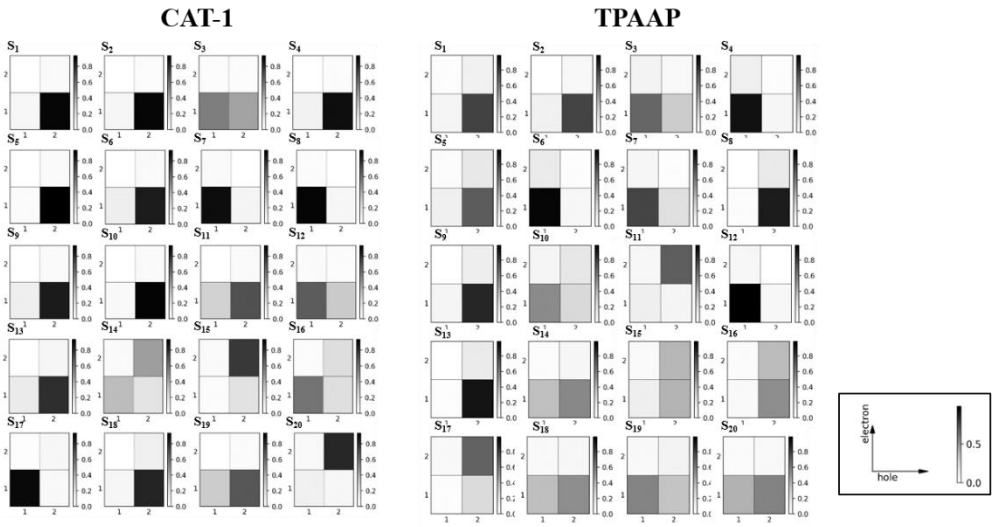

Figure S4. Electron-hole correlation plots of the Omega matrices for the individual states for two molecules. The first 20 excited states are included to find out the excitation process for CAT-1 (in the left) and TPAAP (in the right).

Figure S4 shows all the first 20 excitations of CAT-1 and TPAAP. The acceptor and donor units are labeled by 1 and 2, respectively. As a first option, an electron could be transferred from donor unit 2 to acceptor unit 1, yielding an electron transfer (ET) state in S1 of CAT-1 and TPAAP. Alternatively, the excitation may be entirely localized on an individual acceptor 1, as exemplified in S7 of CAT-1 and S6 of TPAAP. A third option is a case where local excitations on individual fragment are coupled to yield a delocalized state, denoted as a Frenkel exciton in S15 of CAT-1 and S11 of TPAAP, such a Frenkel exciton is shown for a case where the dominant contribution is on the central Donor 2, and the central Acceptor 1 plays a secondary role, while it still plays a less important role in a linear combination from Donor to Acceptor yielding an electron transfer state.

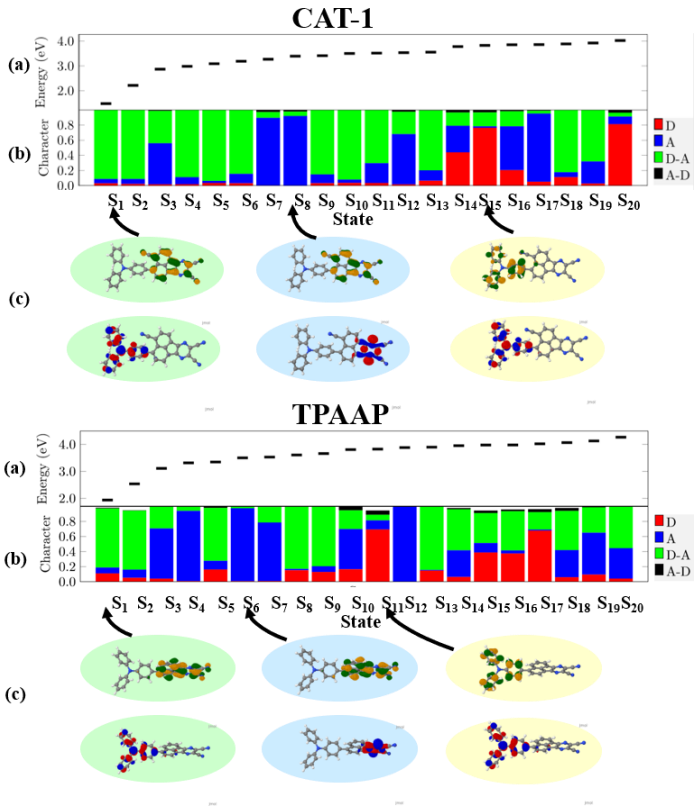

Figure S5. Fragment-based analysis of excited-states of CAT-1 and TPAAP. (a) excited-state character (b) automatically assigned using the ET numbers; and exemplary NTOs (c) of CAT-1 in the S_1, S_8, and S_{15} states; exemplary NTOs of TPAAP in the S_1, S_6, and S_{11} states.

As shown in Figure S5, we also compute the ET numbers with respect to D and A (the Donor and Acceptor fragments, respectively) and group them into the following four contributions: (i) the local excitation on D, (ii) the local excitation on A, (iii) ET from D to A, (iv) ET from A to D. In Figure S5(a), the excitation energies of the first twenty singlet states are shown. The majority admixed with both ET and LE properties; for example, S15 of CAT-1 and S11 of TPAAP are typically the partly localized excitation for donor and a secondary for acceptor, as well as the ET property from donor fragment to acceptor fragment.

4. The dihedral angle Φ of C_1-C_2-C_3-C_4 and its comparison between the ground state and the excited states of two TADF molecules.

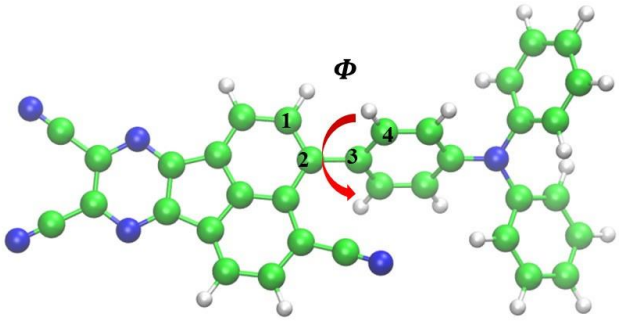

Figure S6. The dihedral angle Φ of C_1-C_2-C_3-C_4 for CAT-1 and TPAAP.

To be more specific, we carefully investigate the photo-absorption property via a fragment-based analysis employed within TheoDORE[3], a toolbox for a detailed and automated analysis of electronic excited state computations. Figure S2 displays the electron-hole correlation, which includes the local excitation of donor and acceptor, respectively, as well as the electron transfer process from donor to acceptor.

Table S1. Comparison of dihedral angle Φ changes between the ground state and the excited states of CAT-1 and TPAAP. The changes refer to the difference between the excited states S_1 and T_1 relative to the ground state S_0.

Molecule	States	Φ(Å)	$\Delta\Phi_{\|Sn\text{-}S0\|}$
CAT-1	S_0	56.5	0
	S_1	89.1	32.6
	T_1	88.7	32.2
TPAAP	S_0	44.6	0
	S_1	57.0	12.4
	T_1	33.3	11.3

The Independent Gradient Model (IGM) analysis[4] is adopted to investigate the weak intermolecular interactions by using the Multiwfn 3.7 package[5,6], as well as the topological properties of the electron density ρ(r) based on atoms in molecules (AIM) theory[7]. The Visual Molecular Dynamics (VMD) visualization program[8] is utilized to render the δg^{inter} isosurface representations. In the IGM method, with the δg^{inter} isosurface map is filled with the $\mathrm{sign}(\lambda_2)\rho$, it can visually describe the corresponding inter−fragment interaction regions and types through various color-filled regions. Theoretically, the IGM descriptor δg represents the difference between IGM type of the true density gradient ($\Delta\rho$) and gradient (Δg^{IGM}), including δg^{intra} and δg^{inter} for exhibiting intra-fragment and inter-fragment interactions, respectively. The descriptors δg and δg^{inter} can be defined as follows:

$$\delta g = \left|\Delta\rho^{\mathrm{IGM}}\right| - \left|\Delta\rho\right|$$

$$\delta g^{\mathrm{inter}} = \left|\Delta\rho^{\mathrm{IGM,inter}}\right| - \left|\Delta\rho\right|$$

where ρ(r) and $\Delta\rho$ represent the electron density with the positive correlation of the bonding strength and electron density gradient vector, respectively. In the Baders AIM theory, the locally aggregated electron density that exhibits attractive interaction can be expressed by the bond critical point (BCP)[5]. Specifically, the topological path can be generated by the connected BCP to show the relationship between bond critical points. In this study, the CN part and H part of the hydrogen bond CN···H are defined as two fragments to draw the isosurface of δg^{inter}.

References

1. Congrave, D. G.; Drummond, B. H.; Conaghan, P. J.; Francis, H.; Jones, S. T. E.; Grey, C. P.; Greenham, N. C.; Credgington, D.; Bronstein, H., A Simple Molecular Design Strategy for Delayed Fluorescence toward 1000 Nm. *J. Am. Chem. Soc.* **2019**, *141*, 18390-18394.

2. Xue, J.; Liang, Q.; Wang, R.; Hou, J.; Li, W.; Peng, Q.; Shuai, Z.; Qiao, J., Highly Efficient Thermally Activated Delayed Fluorescence Via J-Aggregates with Strong Intermolecular Charge Transfer. *Adv. Mater.* **2019**, *31*, 1808242.

3. Plasser, F., Theodore: a Toolbox for a Detailed and Automated Analysis of Electronic Excited State Computations. *J. Chem. Phys.* 2020, **152**, 084108.

4. Ransil, B. J., Studies in Molecular Structure. Iv. Potential Curve for the Interaction of Two Helium Atoms in Single-Configuration Lcao Mo Scf Approximation. *J. Chem. Phys.* **1961**, *34*, 2109-2118.

5. Lu, T.; Chen, F., Quantitative Analysis of Molecular Surface Based on Improved Marching Tetrahedra Algorithm. *J. Mol. Graph. Model.* **2012**, *38*, 314-23.

6. Lu, T.; Chen, F., Multiwfn: A Multifunctional Wavefunction Analyzer. *J. Comput. Chem.* **2012**, *33*, 580-92.

7. Bader, R. F. W., Atoms in Molecules: A Quantum Theory. *J. Mol. Struc-Theochem*, **1994**, *360*.

8. Humphrey, W., Dalke, A. and Schulten, K., VMD --- Visual Molecular Dynamics. *J. Molec. Graph.* **1996**, *14*, 33-38.